Reinvestigation of Metal Ion Specificity for Quinone Cofactor Biogenesis in Bacterial Copper Amine Oxidase[†,‡]

Toshihide Okajima,[*,§] Sei'ichiro Kishishita,[§,||] Yen-Chen Chiu,[§,⊥] Takeshi Murakawa,[§] Misa Kim,[#,▽] Hiroshi Yamaguchi,[#] Shun Hirota,[○] Shun'ichi Kuroda,[§] and Katsuyuki Tanizawa[§]

Department of Structural Molecular Biology, Institute of Scientific and Industrial Research, Osaka University, Ibaraki, Osaka 567-0047, Japan, School of Science and Technology, Kwansei Gakuin University, Sanda, Hyogo 669-1337, Japan, and Department of Physical Chemistry, Kyoto Pharmaceutical University, Kyoto, Kyoto 607-8414, Japan

Received June 6, 2005; Revised Manuscript Received July 25, 2005

ABSTRACT: The topa quinone (TPQ) cofactor of copper amine oxidase is generated by copper-assisted self-processing of the precursor protein. Metal ion specificity for TPQ biogenesis has been reinvestigated with the recombinant phenylethylamine oxidase from *Arthrobacter globiformis*. Besides Cu^{2+} ion, some divalent metal ions such as Co^{2+}, Ni^{2+}, and Zn^{2+} were also bound to the metal site of the apoenzyme so tightly that they were not replaced by excess Cu^{2+} ions added subsequently. Although these noncupric metal ions could not initiate TPQ formation under the atmospheric conditions, we observed slow spectral changes in the enzyme bound with Co^{2+} or Ni^{2+} ion under the dioxygen-saturating conditions. Resonance Raman spectroscopy and titration with phenylhydrazine provided unambiguous evidence for TPQ formation by Co^{2+} and Ni^{2+} ions. Steady-state kinetic analysis showed that the enzymes activated by Co^{2+} and Ni^{2+} ions were indistinguishable from the corresponding metal-substituted enzymes prepared from the native copper enzyme (Kishishita, S., Okajima, T., Kim, M., Yamaguchi, H., Hirota, S., Suzuki, S., Kuroda, S., Tanizawa, K., and Mure, M. (2003) *J. Am. Chem. Soc. 125*, 1041−1055). X-ray crystallographic analysis has also revealed structural identity of the active sites of Co- and Ni-activated enzymes with Cu-enzyme. Thus Cu^{2+} ion is not the sole metal ion assisting TPQ formation. Co^{2+} and Ni^{2+} ions are also capable of forming TPQ, though much less efficiently than Cu^{2+}.

Copper amine oxidase (CAO)[1] (EC 1.4.3.6) contains a redox-active organic cofactor 2,4,5-trihydroxyphenylalanine quinone (topa quinone, TPQ) that is essential for catalyzing the oxidative deamination of various primary amines (*1*−*4*). We have demonstrated with *Arthrobacter globiformis* phenylethylamine oxidase (AGAO) that the TPQ cofactor is post-translationally generated from the precursor tyrosine residue (Tyr382) by a self-catalytic process requiring molecular oxygen and Cu^{2+} ion (*5*−*7*). We have also determined the crystal structures of AGAO in an inactive apo form without TPQ and Cu^{2+} ion and an active holo form containing both of them (*8*). In the apo form structure, the phenolic hydroxyl group of the precursor tyrosine (Tyr382) pointed toward the vacant metal site with the phenoxy oxygen atom of Tyr382 and the imidazole nitrogen atoms of three histidine residues (His431, His433, and His592) arranged in a tetrahedral geometry. In the holo form structure, the nitrogen atoms of the same three histidine residues and a water molecule were placed at an equatorial position, and another water molecule was at an axial position, all coordinating to the Cu^{2+} ion in the distorted square pyramidal geometry (*8*). The TPQ ring was tilted away from the copper site in the "off-copper" conformation. By comparing these structures, conformational changes of the active site residues were predicted to occur during the TPQ biogenesis, which were corroborated recently by time-resolved X-ray crystallography (*9*).

Cu^{2+} ion has so far been believed to be the sole metal ion that can promote the TPQ biogenesis in CAOs (*5*). Thus,

[†] This study was supported by Grants-in-Aid for Scientific Research from the Ministry of Education, Culture, Sports, Science and Technology of Japan (Priority Areas, No. 13125204; the 21st Century Center of Excellence Program) (to K.T.), and from the Japan Society for the Promotion of Science (Category C, No. 14560066) (to T.O.).

[‡] The atomic coordinates and structure factors for the Co- and Ni-enzymes and an initial intermediate of Co-assisted biogenesis of TPQ have been deposited in the Protein Data Bank with the accession codes 1WMN, 1WMO, and 1WMP, respectively.

* To whom correspondence should be addressed. Phone: +81-6-6879-4292. Fax: +81-6-6879-8464. E-mail: tokajima@sanken.osaka-u.ac.jp.

[§] Osaka University.

[||] Current address: Protein Research Group, Genomic Sciences Center, RIKEN Yokohama Institute, Yokohama, Kanagawa 230-0045, Japan.

[⊥] Current address: Department of Exercise and Health Sciences, National Taiwan College of Physical Education, Shuang-shih Road, Taichung 404, the Republic of China (Taiwan).

[#] Kwansei Gakuin University.

[▽] Current address: Institute of Physical and Chemical Research, RIKEN Harima Institute/SPring-8, Mikazuki-cho, Sayo, Hyogo 679-5148, Japan.

[○] Kyoto Pharmaceutical University.

[1] Abbreviations: AGAO, *Arthrobacter globiformis* phenylethylamine oxidase; CAO, copper amine oxidase; Co-AGAO, Co-added (activated) AGAO; Cu-AGAO, Cu-activated AGAO (wild type); HEPES, *N*-(2-hydroxyethyl)piperazine-*N*′-(2-ethanesulfonic acid); HPAO, *Hansenula polymorpha* amine oxidase; LMCT, ligand-to-metal change transfer; Ni-AGAO, Ni-added (activated) AGAO; 2-PEA, 2-phenylethylamine; TPQ, 2,4,5-trihydroxyphenylalanine quinone or topa quinone; TPQ_{ox}, TPQ in the oxidized form; TPQ_{red}, TPQ in the reduced trihydroxybenzene form.

10.1021/bi051070r CCC: $30.25
Published on Web 08/19/2005

metal ions including Mn^{2+}, Co^{2+}, Ni^{2+}, Cd^{2+}, Be^{2+}, Mo^{2+}, Mg^{2+}, Ba^{2+}, Ca^{2+}, and Zn^{2+} ions were all inert for TPQ formation in AGAO (*5*). It has been reported that Zn^{2+} ion is tightly bound to the Cu-binding site of the enzyme from yeast *Hansenula polymorpha* (HPAO) (*10*) and prevents TPQ formation by subsequent incubation with excess Cu^{2+} ions (*11*). Therefore, the metal ion specificity for TPQ biogenesis should be attributed to the intrinsic properties of the bound metal ions, but not to the nature of the proteins, which can bind several kinds of divalent metal ions besides Cu^{2+}.

In further studying the mechanism of TPQ biogenesis in AGAO, we incidentally noticed that the enzyme solution added with Co^{2+} or Ni^{2+} ion, which was initially colorless without TPQ, turned pink on storage in a refrigerator over a month, implying that TPQ was formed. This fortuitous observation led us to reinvestigate the metal ion specificity for TPQ biogenesis. We here demonstrate that Cu^{2+} ion is not the sole metal ion assisting the TPQ formation and that Co^{2+} and Ni^{2+} ions are also capable of forming TPQ in AGAO, though much less efficiently than the native Cu^{2+} ion, requiring a high concentration of dissolved dioxygen.

EXPERIMENTAL PROCEDURES

Materials. Anhydrous $CoCl_2$ (99.999%, w/w) and $NiCl_2 \cdot 6H_2O$ (99.9999%, w/w) were purchased from Aldrich Chemicals. All other chemicals were of the highest grade commercially available and were used without further purification. All buffers were prepared using water with resistance greater than 16.7 MΩ cm, obtained from a NANOpureII system (Barnstead) and further passed over a Chelex column (BIO-RAD). All glass and plastic wares were thoroughly washed with the Chelex-passed water.

Enzyme Purification and Assay. The recombinant AGAO was overproduced in *Escherichia coli* CD03, a catalase-deficient mutant of *E. coli* BL21(DE3) (*12*), carrying the expression vector pEPO-02 and grown in a copper-depleted medium (*5*). The enzyme was purified in an inactive apo form without TPQ and Cu^{2+} ion, as described previously (*5*). The purity was >99% as judged by sodium dodecyl sulfate−polyacrylamide gel electrophoresis, and the purified enzyme had no detectable catalase activity. The enzyme was assayed at 30 °C in 100 mM HEPES buffer (pH 6.8) with 40 μM 2-phenylethylamine (2-PEA) as substrate by the peroxidase-coupled method, as described previously (*5*). Steady-state kinetic parameters were determined on the basis of the ping-pong bi-bi mechanism by changing the concentration of 2-PEA, and calculated by fitting the data to nonlinear regression curves of the Michaelis−Menten equation using Kaleidagraph version 3.0 (Abelbeck Software). Protein concentration was determined spectrophotometrically by using extinction coefficients at 280 nm of 12.3 and 13.2 for 1% (w/v) solutions of the apo and holo forms of AGAO (*5*), respectively. The TPQ and metal contents in the holo AGAO were determined as described previously (*5*).

TPQ Biogenesis with Various Metal Ions. The apo AGAO (0.1 mM subunit, final concentration) was incubated with various metal ions (0.5 mM, as chloride salt), including Ag^{+}, Ba^{2+}, Be^{2+}, Ca^{2+}, Cd^{2+}, Co^{2+}, Cr^{2+}, Cu^{2+}, Fe^{2+}, Hg^{2+}, Mg^{2+}, Ni^{2+}, Pd^{2+}, Rb^{+}, Sn^{2+}, Sr^{2+}, and Zn^{2+}, in 50 mM HEPES (pH 6.8) at 30 °C under aerobic conditions in a cuvette. The reaction was monitored by measuring the spectral changes of enzyme in the wavelength region of 300−800 nm with a UV−vis spectrophotometer. In the cases where noted, the reaction was done in a cuvette tightly sealed with a screw cap and a silicon rubber septum and pressurized with dioxygen through a needle connected to a balloon containing 99.99% O_2 gas. Dissolved oxygen concentration in the reaction mixture measured with a standard Clark-type oxygen electrode was about 1.2 mM at saturation.

Spectroscopic Measurements. UV−vis absorption spectra were recorded at 30 °C with a Hewlett-Packard 8452A diode-array spectrophotometer or a JASCO V-560 UV−vis spectrophotometer. Resonance Raman scattering was excited at 514.5 nm with an Ar^{+} ion laser (Spectra Physics, 2017) and detected with a CCD detector (Princeton Instruments) attached to a triple polychromator (JASCO, NR-1800). The excitation laser beam power was adjusted to 70 mW at the sample point. Measurements were carried out at an ambient temperature with the enzyme solution (about 50 μL) placed in a spinning cell (3000 rpm). The data accumulation time was 200 s. Raman shifts were calibrated with acetone and toluene, and the resolution of the Raman bands was ±1 cm^{-1}.

Crystallization and Data Collection. Holo AGAO, in which TPQ was generated by incubation with Co^{2+} ion (Co-AGAO) or Ni^{2+} ion (Ni-AGAO), was crystallized at 16 °C by the microdialysis method as described previously (*8*, *12*). The protein concentration in the dialysis button (volume, 50 μL) was 10 mg/mL, and the reservoir solution contained 1.05 M potassium sodium tartrate as a precipitant in 25 mM HEPES buffer (pH 6.8). Platelet-like crystals (0.2 × 0.4 × 0.1 mm) appeared within about 2 weeks. The dialysis buttons were then transferred into the same buffer containing 45% (v/v) glycerol as a cryoprotectant. Crystals of apo AGAO were also prepared under the same conditions and soaked in the buffer containing 45% glycerol, which had been thoroughly degassed in an anaerobic glovebox for 1 day. The apo AGAO crystals were further soaked in the same buffer containing 45% glycerol and 5 mM $CoCl_2$ for 16 h before data collection. The crystals were mounted on thin nylon loops (ϕ, 0.2−0.3 mm) and frozen by flash cooling at 100 K in a cold N_2 gas stream.

Diffraction data sets were collected with a synchrotron X-radiation at SPring8 (Hyogo, Japan), at 90 K using an MAR CCD detector in the beam-line station BL44B2 (λ = 0.700 Å) for Co- and Ni-AGAO crystals or at 100 K using an imaging plate DIP6040 (Bruker AXS) in the beam-line station BL44XU (λ = 0.900 Å) for Co-soaked apo AGAO crystals. The collected data were processed, merged, and scaled using Mosflm (*13*) and SCALA (*14*). The three crystals were found to belong to a space group *I2* with the unit cell dimensions that are comparable to those of the wild-type Cu-activated AGAO (Cu-AGAO) at 100 K (*12*). The details and statistics of data collection are summarized in Table 1.

Structural Refinement. The program used for calculation of electron-density maps and simulated-annealing, positional, and *B*-factor refinements was X-PLOR version 3.861 (*15*). Manual rebuilding and assignment of solvent molecules were performed using QUANTA version 97 (Accelrys, San Diego, CA). An initial model for AGAO dimer was generated by 180° rotation around the crystallographic 2-fold axis of the monomer coordinates (PDB code, 1AVK) without solvent molecules. Using the dimer AGAO structure as an initial

Table 1: Statistics of Data Collection and Refinement

	Co-AGAO	Ni-AGAO	Co-soaked apo AGAO
Data Collection			
cell			
space group	*I*2	*I*2	*I*2
unit cell dimens			
a (Å)	157.68	157.68	157.58
b (Å)	63.09	62.99	63.38
c (Å)	184.09	183.67	184.20
β (deg)	111.76	111.84	112.47
no. of observations	685 663	800 590	334 109
no. of unique reflns	184 462	217 340	112 420
$d_{max} - d_{min}$ (Å)	25.1−1.7	22.3−1.6	24.1−2.0
overall completeness (%)	99.7	98.3	98.8
overall R_{merge} (%)[a]	6.1	12.4	9.4
Refinement Statistics			
$d_{max} - d_{min}$ (Å)	10−1.8	10−1.8	10−2.0
residues in the core ϕ, φ regions (%)	88.8	89.0	88.3
no. of non-hydrogen atoms	10,893	10,845	10,709
no. of solvent atoms	1155	1107	975
av temp factors			
main-chain (Å^2)	18.5	18.5	26.5
side-chain atoms (Å^2)	20.1	20.1	28.1
solvent atoms (Å^2)	31.4	30.5	38.1
rms deviation from ideal values			
bond lengths (Å)	0.010	0.010	0.006
bond angles (deg)	1.8	1.9	1.3
residual *R* (%)[b]	22.4	22.3	18.8
free residual *R* (%)[c]	27.0	26.6	22.0

[a] $R_{merge} = \sum h \sum i |I_{h,i} - \langle I_h \rangle| / \sum h \sum i I_{h,i}$, where $I_{h,i}$ is the intensity value of the *i*th measurement of *h* and $\langle I_h \rangle$ is the corresponding mean value of I_h for all *i* measurements. [b] $R = \sum ||F_o| - |F_c|| / \sum |F_o|$. [c] Free residual *R* is an *R* factor of the refinement evaluated for 5% of reflections that were excluded from the refinement.

model, electron density maps were calculated after rigid-body refinement. The structures obtained for Co- and Ni-AGAO and Co-soaked apo AGAO crystals were further refined through simulated annealing at 3000 K and several cycles of positional and *B*-factor refinements. Metal ions were assigned on the basis of the highest peaks in the respective $2F_o - F_c$ maps; water molecules and residues in the active site region were carefully modeled using the $2F_o - F_c$, $F_o - F_c$, and omit maps. The details and statistics of crystallographic refinement for Co- and Ni-AGAO and Co-soaked apo AGAO structures are also given in Table 1.

RESULTS

Binding of Various Metal Ions. We previously investigated the metal ion specificity for self-catalytic formation of the TPQ cofactor in AGAO and found that only Cu^{2+} ion among various metal ions tested was able to generate TPQ (*5*). We interpreted that the metal ions other than Cu^{2+} ion might be inactive simply because they were not bound to the specific metal-binding site of AGAO. To examine this possibility, the metal-free apo AGAO was first incubated with various metal ions (0.5 mM Ag^+, Ba^{2+}, Be^{2+}, Ca^{2+}, Cd^{2+}, Co^{2+}, Cr^{2+}, Fe^{2+}, Hg^{2+}, Mg^{2+}, Ni^{2+}, Pd^{2+}, Rb^+, Sn^{2+}, Sr^{2+}, or Zn^{2+}) at 30 °C for 24 h, and further incubated after addition of 0.5 mM Cu^{2+} ion. In the initial 24 h incubation, there was no increase in the absorption at 480 nm due to TPQ, corroborating that all metal ions besides Cu^{2+} are inert for TPQ generation as described previously (*5*). If the preadded metal ion is not bound or only weakly bound to the metal site of AGAO and is therefore readily replaced by Cu^{2+} ion added subsequently, the TPQ generation reaction should be immediately initiated by the addition of Cu^{2+} ion. Metal ions including Ag^+, Ba^{2+}, Be^{2+}, Ca^{2+}, Cd^{2+}, Cr^{2+}, Fe^{2+}, Hg^{2+}, Mg^{2+}, Pd^{2+}, Rb^+, Sn^{2+}, and Sr^{2+} ions were found to belong to this group; the Cu^{2+} ion added later promoted TPQ generation in a manner similar to that without preaddition of noncupric metal ions (Figure 1). Mn^{2+} ion appeared to be bound to AGAO to a certain extent, as the TPQ generation was significantly retarded, probably following slow exchange with the subsequently added Cu^{2+} ion. In marked contrast, preincubation with either Co^{2+}, Ni^{2+}, or Zn^{2+} ion resulted in yielding the enzyme that could not form TPQ by the subsequent addition of excess Cu^{2+} ion, indicating that those latter three metal ions were bound so tightly to the Cu-binding site of AGAO that they were not replaced by Cu^{2+} ion added later. Alternatively, their binding to another site may somehow prevent the specific binding of Cu^{2+} ion or initiating the TPQ biogenesis by, for example, indirect conformational changes of the active site. However, it seemed more likely that the Cu-binding site of AGAO constituted by three histidine residues (His431, His433, and His592; vide infra) could bind not only Cu^{2+} ion but also other metal ions such as Co^{2+}, Ni^{2+}, and Zn^{2+} ions, which were apparently inert for TPQ biogenesis.

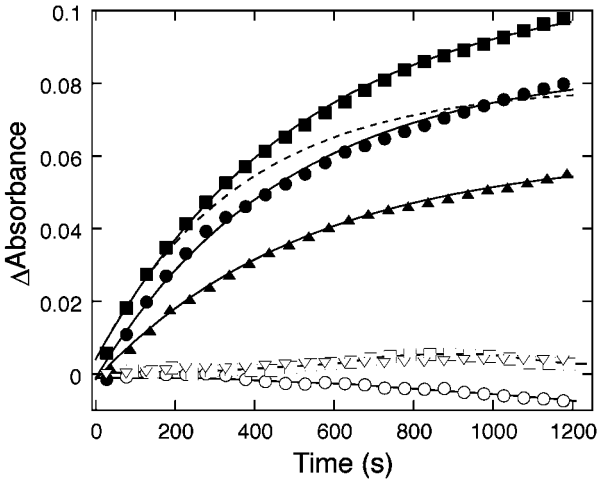

FIGURE 1: Binding assay for various metal ions. Apo AGAO (0.1 mM subunit) was preincubated with 0.5 mM Co^{2+}(□), Ni^{2+}(▽), Zn^{2+}(○), Ca^{2+}(●), Mg^{2+}(■), or Mn^{2+}(▲) at 30 °C for 24 h, and after further addition of 0.5 mM Cu^{2+} the absorbance changes at 480 nm were monitored. (- - -) Without preincubation with a noncupric ion.

TPQ Biogenesis Assisted by Co^{2+} and Ni^{2+} Ions. It was rather fortunate that we did not discard the above enzyme samples added with various noncupric metal ions and kept them in a refrigerator over a month until we noticed that two of them colored pink, implying the formation of TPQ. The two colored samples were those added with Co^{2+} and Ni^{2+} ions but without a second addition of Cu^{2+} ion. We suspected that Co^{2+} and Ni^{2+} ions were also able to assist TPQ generation, albeit extremely inefficiently. Since the TPQ biogenesis reaction is an oxidative modification of the precursor tyrosine residue (Tyr382) and depends on the concentration of dissolved oxygen (*16*), we then attempted to accelerate the Co^{2+}/Ni^{2+} ion-assisted TPQ biogenesis by using a high concentration of dissolved oxygen ($[O_2]$ at saturation = ca. 1.2 mM). As shown in Figure 2A and Figure 2B, we could indeed observe slow spectral changes upon addition of 0.5 mM Co^{2+} or Ni^{2+} ion in a measurable time

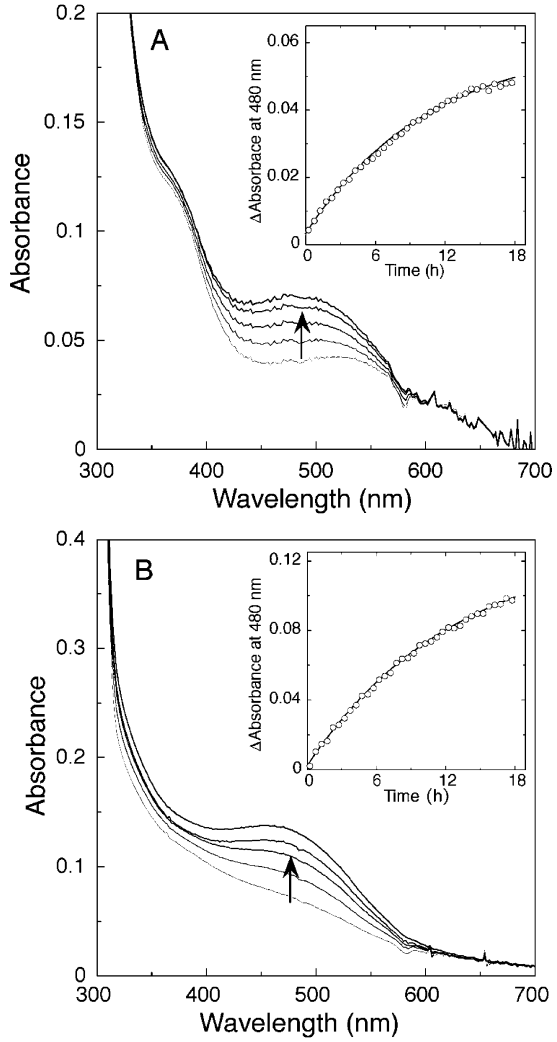

FIGURE 2: Spectral changes during incubation with Co^{2+} and Ni^{2+} ions under O_2-saturating conditions. Apo AGAO (0.1 mM subunit) was incubated at 30 °C with 0.5 mM Co^{2+} (A) or Ni^{2+} (B) under O_2-saturating conditions ($[O_2] = \sim 1.2$ mM). Absorption spectra were recorded at 0, 3, 6, 9, 12, 15 h; arrows indicate the direction of the spectral changes. Insets: Absorbance changes at 480 nm were plotted against incubation time and fitted to pseudo-first-order kinetics by the least-squares method (see Table 2).

Table 2: Rates of TPQ Biogenesis Assisted by Cu^{2+}, Co^{2+}, and Ni^{2+} Ions

metal ion	biogenesis rate[a] (min^{-1})
$Cu^{2+} = 0.5$ mM	1.50 ± 0.2
$Co^{2+} = 0.5$ mM	$(1.32 \pm 0.04) \times 10^{-3}$
$Co^{2+} = 0.5$ mM, $Cu^{2+} = 0.005$ mM	$(1.36 \pm 0.05) \times 10^{-3}$
$Ni^{2+} = 0.5$ mM	$(1.25 \pm 0.02) \times 10^{-3}$
$Ni^{2+} = 0.5$ mM, $Cu^{2+} = 0.005$ mM	$(1.18 \pm 0.02) \times 10^{-3}$
$Ni^{2+} = 0.5$ mM, $Cu^{2+} = 0.05$ mM	$(1.41 \pm 0.03) \times 10^{-3}$

[a] Determined from the increase in absorbance at 480 nm at 30 °C and pH 6.8. Averaged values of two independent measurements are shown.

scale (<18 h). The high concentration of dissolved oxygen was needed for initiating such observable spectral changes. The absorption maximum at about 480 nm corresponds to λ_{max} of the oxidized form of TPQ (TPQ_{ox}) in AGAO (*5*). Pseudo-first-order rate constants (k_{obs}) estimated from the increase in absorbance at 480 nm (Figure 2, insets) are given in Table 2. The k_{obs} values for Co^{2+} and Ni^{2+} ions are about 1200-fold smaller than that for Cu^{2+} ion measured under the conditions saturated with dissolved dioxygen.

We have purchased the chloride salts of metal ions ($CoCl_2$ and $NiCl_2$) of the highest purity commercially available (99.999%, w/w). Nevertheless, we cannot exclude a possibility of TPQ generation by a trace contaminating Cu^{2+} ion in the solution of Co^{2+} and Ni^{2+} ions. To examine this, a small amount of Cu^{2+} ion (final concentration, 0.005 or 0.05 mM), far exceeding the upper limit of contamination (0.001%, w/w), was added intentionally to the above metal solutions and the rates of TPQ generation (k_{obs}) were measured by the increase in absorbance at 480 nm (Table 2). Intentional addition of a small amount of Cu^{2+} ion had essentially no effect on the rates of TPQ generation by Co^{2+} and Ni^{2+} ions, clearly showing that the slow generation of TPQ by Co^{2+} and Ni^{2+} ions is not due to a trace contaminating Cu^{2+} ion, if any.

Characterization of Co- and Ni-AGAO. To identify the chromophore formed in the Co- and Ni-added AGAO (Co- and Ni-AGAO), the apoenzyme was incubated with 0.5 mM Co^{2+} or Ni^{2+} ion at 30 °C for 72 h under the conditions saturating with dioxygen ($[O_2] = 1.2$ mM) and then dialyzed extensively against 25 mM HEPES buffer (pH 6.8) containing 4 mM EDTA. Metal contents determined by atomic absorption spectrometry revealed nearly stoichiometric incorporation of each metal ion, as well as less than 1% contamination of copper (Table 3). Absorption spectra of Co- and Ni-AGAO shown in Figure 3A agreed well with that of Cu-AGAO, having the molar absorption coefficient of about 1800 M^{-1} cm^{-1} (λ_{max} at 480 nm). Resonance Raman spectra of Co- and Ni-AGAO were also very similar to that of Cu-AGAO with characteristic vibrational modes derived from TPQ_{ox}, such as stretching modes of the C2═O and C5═O carbonyl groups at 1575 cm^{-1} and 1686 cm^{-1}, respectively (*17*), together with other lower energy modes observed in the 1200−1400 cm^{-1} region (C═C and C−C stretching and C−H bending motions) (Figure 3B). The amounts of TPQ_{ox} in Co- and Ni-AGAO, as determined by titration with phenylhydrazine, were comparable with those of the holo Cu-AGAO (Table 3). Altogether, these data unequivocally show that the chromophore formed in Co- and Ni-AGAO is TPQ.

Despite the cofactor formation, Co- and Ni-AGAO showed very low catalytic activities (Table 3). This is consistent with the previous finding that the native Cu^{2+} ion is required not only for the cofactor biogenesis but also for the catalytic activity (*12*, *18*). Also shown in Table 3 are the steady-state kinetic parameters of Cu-, Co-, and Ni-AGAO. K_m values for 2-PEA of Co- and Ni-AGAO were similar to that of the native Cu-enzyme. In contrast, k_{cat} values of Co- and Ni-AGAO, determined with a saturated concentration of 2-PEA, were considerably lower, suggesting that the bound metal ion participates in the catalytic process, rather than in the substrate binding. We have recently investigated the catalytic role of Cu^{2+} ion by replacing with various metal ions and proposed that the bound metal ion provides a binding site for the reduced dioxygen species to be efficiently protonated and released during the oxidative half-reaction of the catalytic cycle (*12*). The low k_{cat} values of Co- and Ni-AGAO are comparable with those of the Co- and Ni-substituted enzymes, prepared by metal substitution of the native Cu-enzyme (*12*), and this result is consistent with the key role of Cu^{2+} ion in the oxidative half-reaction.

Table 3: Characteristics of AGAO Activated by Cu^{2+}, Co^{2+}, and Ni^{2+} Ions

enzyme	sp act. (U/mg)	TPQ content (mol/subunit)	metal content[a] (mol atom/subunit)	K_m for 2-PEA (μM)	k_{cat} (s^{-1})
Cu-AGAO	67.5	0.68 ± 0.01	0.88 ± 0.0015 (Cu)	2.5 ± 0.03	75.7 ± 0.8
Co-AGAO	0.35	0.51 ± 0.0002	0.0082 ± 0.00056 (Cu) 1.12 ± 0.0032 (Co)	2.5 ± 0.3	0.92 ± 0.02
Ni-AGAO	0.23	0.58 ± 0.0008	0.0065 ± 0.00062 (Cu) 0.93 ± 0.011 (Ni)	3.4 ± 0.4	0.63 ± 0.02

[a] Determined for the metals indicated in parentheses.

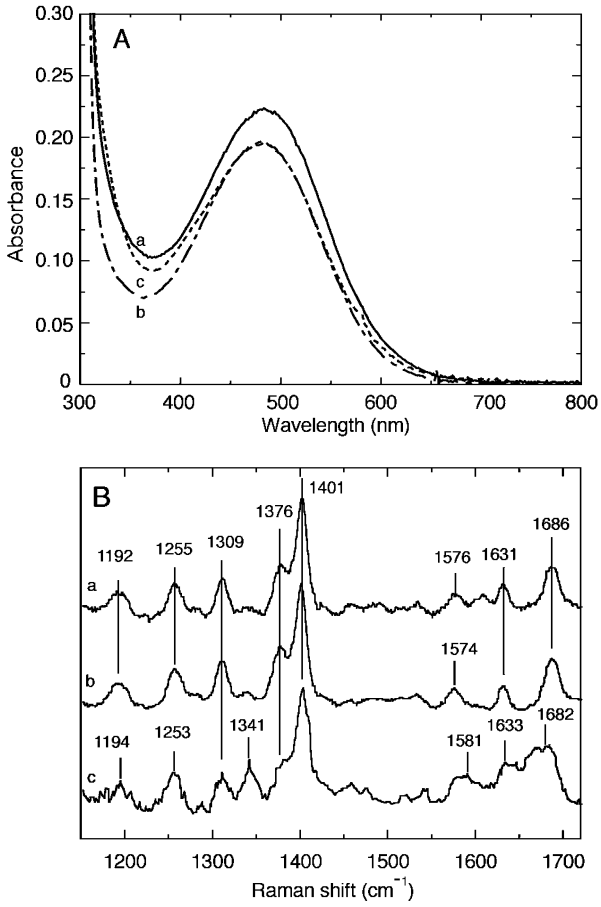

FIGURE 3: UV−vis absorption and resonance Raman spectra of Co-, Ni-, and Cu-AGAO. Absorption (A) and resonance Raman (B) spectra of Co-AGAO (a), Ni-AGAO (b), and Cu-AGAO (c) were measured in 50 mM HEPES, pH 6.8, at a subunit concentration of 0.1 mM. Raman shifts (wavenumbers) calibrated with acetone and toluene standards (not shown) are indicated above the peaks.

X-ray Crystallographic Structures of Co- and Ni-AGAO. To structurally compare with the native Cu-AGAO, X-ray crystallographic structures were determined for Co- and Ni-AGAO (Table 1). The overall polypeptide folds of Co- and Ni-AGAO were essentially identical with that of the wild-type Cu-AGAO, giving root-mean-square deviations of about 0.5 Å for the coordinates of all main-chain atoms. Most side chains in the Co- and Ni-AGAO structures also maintain the same conformations as those in the Cu-AGAO structure. In the active sites of Co- and Ni-AGAO, $F_o - F_c$ omit maps contoured at $\pm 4.0\sigma$ for residue 382 clearly show that the phenolic side chain has extra electron densities at both of the C2 and C5 positions. Thus, in agreement with the spectroscopic data described above, X-ray structures also revealed that residue 382 had been fully processed to the TPQ cofactor (Figure 4A and Figure 4B). The modeled TPQ cofactors in Co- and Ni-AGAO are both in an "off-copper" conformation, as shown previously in the active form of Cu-AGAO (*8*). As for the metal coordination structure, the Cu^{2+} ion in Cu-AGAO is 5-coordinated with 3 imidazole nitrogen atoms of His residues (His431, His433, and His592) and 2 oxygen atoms of water molecules arranged in a distorted square pyramidal geometry (*8*). The bound Co^{2+} and Ni^{2+} ions in Co- and Ni-AGAO occupy the same metal site as the Cu^{2+} ion in the native Cu-enzyme, but are 6-coordinated in an octahedral geometry with 3 imidazole nitrogen atoms of the same His residues and 3 oxygen atoms of water molecules (Wa1, Wa2, and Wa3) (Figure 4A and Figure 4B). This octahedral metal-coordination geometry has also been observed previously in the structures of Co- and Ni-AGAO prepared by metal substitution (*12*).

Furthermore, to structurally visualize the initial stage of the Co^{2+} ion-assisted biogenesis of TPQ, apo AGAO crystals were soaked anaerobically in the buffer containing 5 mM $CoCl_2$ and subjected to X-ray diffraction studies. As expected, a strong electron density, assignable to the bound Co^{2+} ion, was observed in the metal-binding site of AGAO. An $F_o - F_c$ omit map contoured at $\pm 4.0\sigma$ clearly shows that Tyr382 remains unprocessed with its 4-hydroxyl group pointing toward the Co^{2+} ion (Figure 4C). The distance between O-4 atom of Tyr382 and the bound Co^{2+} ion is about 2.6 Å, which is not close enough to allow a ligand-to-metal change transfer (LMCT). The coordination structure of the Co^{2+} ion is a trigonal pyramid, consisting of 3 imidazole nitrogen atoms of His residues (His431, His433, and His592) and the phenolic oxygen atom of Tyr382. There is no water molecule directly bound to the Co^{2+} ion. Thus, the metal coordination structure of the Co-soaked apo AGAO is essentially identical with that of the initial structure formed during the Cu-assisted TPQ biogenesis (bio-1; PDB code, 1IVU) (*9*). These results strongly suggest that the mechanism of the metal ion assisted TPQ biogenesis in AGAO is essentially the same with Cu^{2+}, Co^{2+}, and probably Ni^{2+} ions, but differs only in the overall rates of the TPQ generation as described above ($Cu^{2+} \gg Co^{2+} \geq Ni^{2+}$, see Table 2).

DISCUSSION

We have clearly shown here for the first time that generation of the TPQ cofactor in a CAO is assisted not only specifically by Cu^{2+} ion but also by some other noncupric metal ions, such as Co^{2+} and Ni^{2+}, though extremely inefficiently as compared with the native Cu^{2+} ion. Seventeen metal ions examined for TPQ generating activity in the present study are classified into three groups: (1) Cu^{2+}, Co^{2+}, and Ni^{2+}, which are tightly bound to the specific metal-binding site and are capable of promoting the TPQ biogenesis; (2) Zn^{2+}, which is also tightly bound to the site (i.e.,

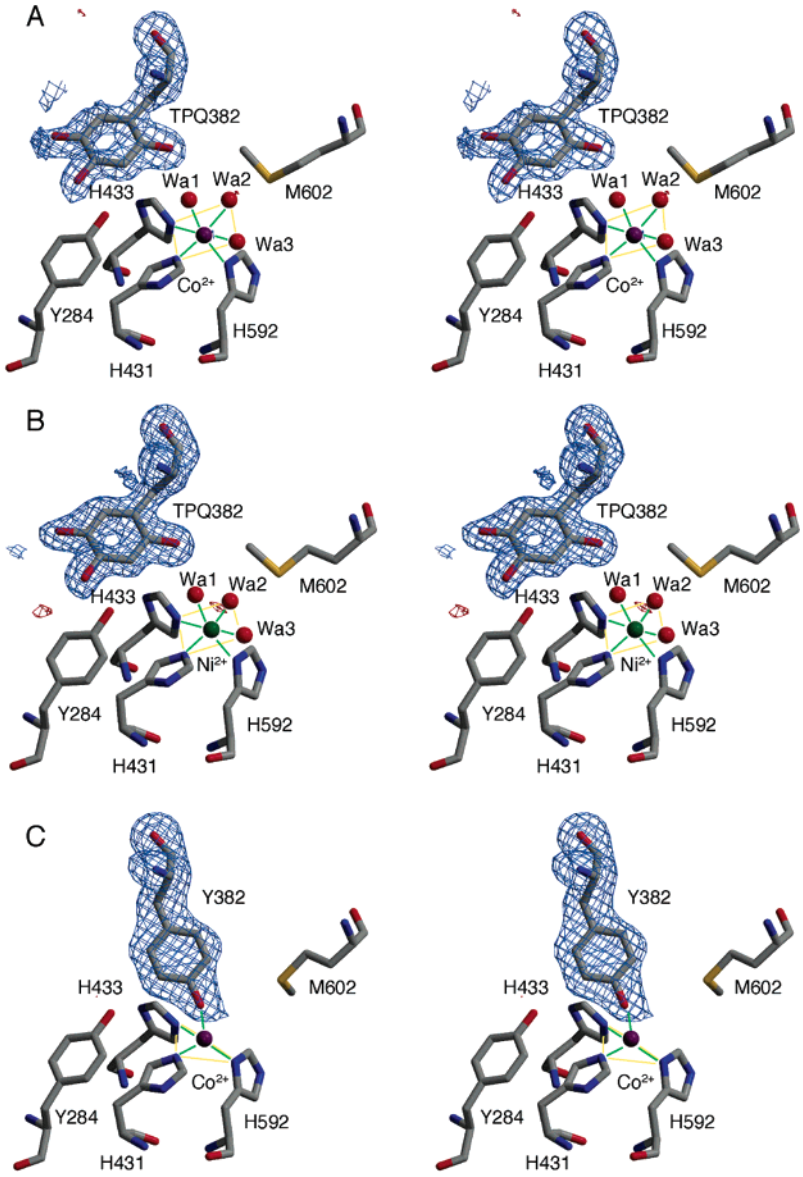

FIGURE 4: Stereoviews of the active-site structures of Co- and Ni-AGAO. The annealed $F_o - F_c$ omit maps (A, Co-AGAO; B, Ni-AGAO; C, Co-soaked apo AGAO) for residue 382 were contoured at 4.0σ (blue) and at $-$ 4.0σ (red) and are shown with the final models. To emphasize the metal coordination geometry, the ligands and metal ion are connected by yellow and green lines.

unexchangeable with excess Cu^{2+} ion added later) but is inert for TPQ generation; (3) others which are not or only weakly (e.g., Mn^{2+}) bound and are incapable of generating TPQ. We cannot provide at the moment an appropriate rationale for the metal ion specificity for binding to the specific site of AGAO, commonly applicable to those belonging to groups 1 and 2 (Cu^{2+}, Co^{2+}, Ni^{2+}, and Zn^{2+}). Presumably, however, they might have a proper ionic radius (not too small or large) that can be accommodated within the cavity of the metal center and also an ability to form a specific, stable metal coordination structure with the protein ligands (His431, His433, His592, and Tyr382) with or without a few molecules of H_2O. Also, it is unknown why only the three metal ions (Cu^{2+}, Co^{2+}, and Ni^{2+}) are able to assist the TPQ biogenesis, but intrinsic properties of the bound metal ions, such as Lewis acidity, may account for their TPQ-generating abilities as discussed later.

Based on the time-resolved X-ray crystallographic studies on the process of Cu-assisted TPQ biogenesis in AGAO (*9*), we have proposed a mechanism of TPQ generation including three possible intermediates: a Tyr/Cu^{2+} complex (not necessarily an LMCT complex) (*19*), dopa quinone, and TPQ in the reduced trihydroxybenzene form (TPQ_{red}). Extensive kinetic studies using yeast HPAO have also proposed a mechanism in which a rate-limiting step in the overall TPQ generation in HPAO is the reaction of the Cu^{2+}-activated precursor Tyr residue with dioxygen prebound at a nonmetal site (*20*, *21*). A linear relationship observed between the dissolved O_2 concentration and the rate of TPQ generation suggested that the affinity for O_2 of the nonmetal binding site is rather low (*21*). The rate of Cu^{2+}-assisted TPQ generation in AGAO, as well, increased linearly with the concentration of dissolved O_2 (Chiu et al., unpublished data). If there is an O_2-prebinding site in AGAO located in some distance from the metal center as proposed for HPAO (*21*), it is unlikely that the [O_2] dependency of the rate of TPQ generation is affected so significantly by the kind of bound metal ions. As demonstrated here, saturating concentrations ($\sim$1.2 mM) of dissolved O_2 are needed for the Co^{2+}/Ni^{2+} ion-assisted generation of TPQ to proceed at an observable

rate. Thus the initial reaction of the precursor Tyr residue with O_2 may be a bimolecular collision, being linearly dependent on the dissolved [O_2]. It appears that the reactivity of the metal-activated Tyr toward O_2 depends primarily on the intrinsic properties of metal ions with the native Cu^{2+} ion activating most efficiently.

As reported previously in the metal substitution studies on AGAO (*12*), the metal-free TPQ_{red} form of AGAO prepared by reduction with dithionite followed by removal of Cu^+ by treatment with cyanide and extensive, anaerobic dialysis can be reoxidized to the active TPQ_{ox} form by reconstitution with Cu^{2+}, Co^{2+}, and Ni^{2+} ions, but not with Zn^{2+} ion. The observed rates of oxidation of TPQ_{red} by Cu^{2+}, Co^{2+}, and Ni^{2+} ions are 1.0, 0.57, and 0.065 min^{-1}, respectively, at 30 °C, pH 6.8, and at an ambient oxygen concentration (*12*), indicating that the metal ion specificity for this step is less strict than that for the overall TPQ biogenesis with the k_{obs} values of biogenesis assisted by the three metal ions differing by about 1200-fold, as described above. TPQ_{red} is also an intermediate immediately preceding the final TPQ_{ox} in the proposed mechanism of TPQ biogenesis in AGAO (*9*). Interestingly, these three metal ions are common to those that can initiate the TPQ biogenesis reported here. Therefore, in the TPQ biogenesis the metal ions are required for both the initial oxidative modification (oxygenation) of the precursor Tyr phenol ring and the final 2-electron oxidation of TPQ_{red} to TPQ_{ox}. Metal ion requirement for the latter process has also been demonstrated in a very recent study of divalent metal ion assisted water addition reaction to a dopa quinone model compound forming the TPQ-like corresponding hydroxyquinone ($Cu^{2+} \gg Zn^{2+} \geq Ni^{2+}$) (*22*). More importantly, the same three metal ions are also necessary for the catalytic activity, playing essential roles particularly in the oxidative half-reaction (*12*). While Zn^{2+} ion is again inert for the catalytic activity of AGAO, the difference in the catalytic rates of the native Cu^{2+}-enzyme and the Co^{2+}- and Ni^{2+}-reconstituted enzymes is only 70−100-fold (*12*) (see also Table 3).

Among physicochemical properties of divalent metal ions, Lewis acidity may account for the different activities of the three metal ions assisting the TPQ generation. When pK_a values of a metal-coordinating water are taken as an assessment of Lewis acidity of metal ions, Cu^{2+} ion (pK_a = 7.5) has a value two pH units lower than that of Co^{2+} (pK_a = 9.6) and Ni^{2+} (pK_a = 9.4) ions (*23*); Cu^{2+}-coordinating water is 100-fold more dissociated than those coordinating to Co^{2+} and Ni^{2+} at neutral pH. The initial intermediate in the TPQ biogenesis is probably the precursor Tyr (Tyr382 in AGAO) with its 4-OH group axially coordinating to the bound Cu^{2+} ion (*9*). Although the distance (2.5 Å) between the O-4 atom of Tyr382 and bound Cu^{2+} ion estimated from the crystal structure is not short enough for an LMCT interaction, the higher Lewis acidity of Cu^{2+} ion would be advantageous for activation of the Tyr phenol ring to a partially electron-deficient state through the O-4 atom. Formation of a Tyr radical ($Tyr^{\bullet}$) by full $1e^-$-transfer to Cu^{2+} may also allow the facile reaction of Cu^{1+} with O_2 yielding superoxide (O_2^-), which then reacts readily with $Tyr^{\bullet}$, but this is only feasible with Cu^{2+}; $1e^-$-reduction of Co^{2+} and Ni^{2+} to Co^{1+} and Ni^{1+}, respectively, is energetically unlikely because of their very low reduction potentials. The redox role of metals also appears to be ruled out in view of the recent observation that TPQ is generated in the Cu^{1+}-added precursor form of HPAO at a rate even 16-fold slower than in the Cu^{2+}-added form, suggesting that Cu^{1+} must be first oxidized to Cu^{2+} by O_2 to initiate the efficient TPQ generation (*24*).

However, the Lewis acidity of metals alone does not explain the inability of Zn^{2+} ion for TPQ generation [and also for catalyzing amine oxidation in AGAO (*12*)]; the pK_a value of Zn^{2+}-coordinating water (pK_a = 9.6) is comparable with that of Co^{2+}-coordinating water. Therefore, despite much less favorable redox potentials of Co^{2+} and Ni^{2+} for $1e^-$-reduction compared to Cu^{2+}, the redox nature of metals may still be a component of the mechanism of TPQ biogenesis, as the redox inactive Zn^{2+} ion does not support biogenesis. A very recent review article has also provided an unpublished observation that the redox active Ni^{2+} ion, but not the inactive Zn^{2+} ion, can support TPQ biogenesis in HPAO (*24*). Provided that the previously proposed mechanism that involves a redox change of Cu^{2+} to Cu^{1+} (*8*) is operative in the copper-assisted TPQ biogenesis, another possibility that a different, but much less efficient, metal mediated mechanism without involving a redox change occurs in the case of Co^{2+} and Ni^{2+} ions also cannot be ruled out.

Alternatively, the metal ion specificity may somehow be associated with the versatility of the coordination structure afforded by each metal ion, as typically observed during the Cu^{2+}-assisted process of the TPQ generation in AGAO (*9*). The Cu^{2+} ion bound initially to the precursor form of AGAO in the absence of O_2 is coordinated in a trigonal pyramid geometry with 4 ligands including 3 imidazole nitrogen atoms of His residues (His431, His433, and His592) and the 4-hydoxyl oxygen atom of Tyr382 (precursor to TPQ), whereas it is coordinated in a distorted square pyramidal geometry with 5 ligands (the same 3 His residues and 2 water molecules) in the mature TPQ-containing active form (*9*). This versatility of the Cu^{2+}-coordination structure is mainly provided by the conformational flexibility of His592 (*19*). It is interesting to note that the affinity for anion (e.g., azide) of the Cu^{2+} ion bound to apo HPAO in the absence of O_2 is 2 orders of magnitude greater than the same Cu^{2+} ion in the mature enzyme in the presence of O_2 (*25*). The anionic affinity of metal is closely related to its Lewis acidity. Therefore, if the coordination structures of the bound Cu^{2+} ion in the apo and mature forms of HPAO are analogous to those in the corresponding forms of AGAO, this observation suggests that the Lewis acidity is affected significantly by the metal coordination structure. Thus the much stronger anion affinity (=Lewis acidity) of Cu^{2+} ion bound to apo HPAO, likely reflecting the role of Cu^{2+} ion in activating the precursor Tyr, may be attained in combination with its trigonal pyramid geometry. Although the Co^{2+} ion (and presumably Ni^{2+}) bound to apo AGAO has a coordination structure similar to Cu^{2+} as described above, its Lewis acidity may be too weak to efficiently activate the precursor Tyr. However, the metal coordination structure again fails to explain the inability of Zn^{2+} ion for TPQ generation, as the Zn^{2+} ion bound to apo HPAO is 4-coordinated in a trigonal pyramid geometry like the Cu^{2+} and Co^{2+} ions bound to apo AGAO (*10*).

In conclusion, the present studies have demonstrated that common divalent metal ions are required for both the self-

processing generation of the TPQ cofactor and the catalytic activity of AGAO. Although there is a marginal but noticeable difference in the metal ion specificity for catalysis among CAOs from different sources [e.g., the Co^{2+}-substituted form of HPAO catalyzes amine oxidation with nearly the same k_{cat} as the wild-type Cu^{2+}-containing form (*26*), while the same metal form of AGAO possesses only 2% k_{cat} of Cu^{2+}-AGAO (*12*)], Cu^{2+} is the best metal ion that efficiently promotes both the TPQ biogenesis and catalysis for all CAOs. If the metal ion specificities for TPQ biogenesis (1200-fold) and catalysis (70−100-fold) are combined, Cu^{2+} ion is about 100000-fold preferred by AGAO to Co^{2+} and Ni^{2+} ions. Although Co^{2+} and Ni^{2+} ion-assisted TPQ biogenesis demonstrated here may be biologically insignificant because of the requirement of such a high concentration of dissolved O_2, the markedly high preference for Cu^{2+} ion well rationalizes the natural selection of this particular metal among those (Co^{2+}, Cu^{2+}, Ni^{2+}, and Zn^{2+}) showing similar natural abundance. Also, we would like to emphasize that comparative studies using various metal ions as employed here can only provide a clue to answer a general question, "why is copper, not other metals, used in copper proteins?", or a more specific one, "what property of copper is most important for TPQ biogenesis and catalysis of copper amine oxidase?" An answer for the latter question may be its high Lewis acidity exhibited in cooperation with the coordination structure in the protein.

REFERENCES

1. Klinman, J. P., and Mu, D. (1994) Quinoenzymes in biology, *Annu. Rev. Biochem. 63*, 299−344.
2. McIntire, W. S., and Hartmann, C. (1993) Copper-containing amine oxidases, in *Principles and Applications of* Quinoproteins (Davidson, V. L., Ed.) pp 97−171, Marcel Dekker, New York.
3. Knowles, P. F., and Dooley, D. M. (1994) Amine oxidases, in *Metal Ions in Biological Systems* (Sigel, H., and Sigel, A., Eds.) Vol. 30, pp 361−403, Marcel Dekker, New York.
4. Janes, S. M., Mu, D., Wemmer, D., Smith, A. J., Kaur, S., Maltby, D., Burlingame, A. L., and Klinman, J. P. (1990) A new redox cofactor in eukaryotic enzymes: 6-hydroxydopa at the active site of bovine serum amine oxidase, *Science 248*, 981−987.
5. Matsuzaki, R., Fukui, T., Sato, H., Ozaki, Y., and Tanizawa, K. (1994) Generation of the topa quinone cofactor in bacterial monoamine oxidase by cupric ion-dependent autooxidation of a specific tyrosyl residue, *FEBS Lett. 351*, 360−364.
6. Cai, D., and Klinman, J. P. (1994) Copper amine oxidase: heterologous expression, purification, and characterization of an active enzyme in *Saccharomyces cerevisiae*, *Biochemistry 33*, 7647−7653.
7. Cai, D., and Klinman, J. P. (1994) Evidence of a self-catalytic mechanism of 2,4,5-trihydroxyphenylalanine quinone biogenesis in yeast copper amine oxidase, *J. Biol. Chem. 269*, 32039−32042.
8. Wilce, M. C. J., Dooley, D. M., Freeman, H. C., Guss, J. M., Matsunami, H., McIntire, W. S., Tanizawa, K., and Yamaguchi, H. (1997) Crystal structures of the copper-containing amine oxidase from *Arthrobacter globiformis* in the holo and apo forms: Implications for the biogenesis of topaquinone, *Biochemistry 36*, 16116−16133.
9. Kim, M., Okajima, T., Kishishita, S., Yoshimura, M., Kawamori, A., Tanizawa, K., and Yamaguchi, H. (2002) X-ray snapshots of quinone cofactor biogenesis in bacterial copper amine oxidase, *Nat. Struct. Biol. 9*, 591−596.
10. Chen, Z., Schwartz, B., Williams, N. K., Li, R., Klinman, J. P., and Mathews, F. S. (2000) Crystal sructure at 2.5 Å resolution of zinc-substituted copper amine oxidase of *Hansenula polymorpha* expressed in *Escherichia coli*, *Biochemistry 39*, 9709−9717.
11. Cai, D., Williams, N. K., and Klinman, J. P. (1997) Effect of metal on 2,4,5-trihydroxyphenylalanine (topa) quinone biogenesis in the *Hansenula polymorpha* copper amine oxidase, *J. Biol. Chem. 272*, 19277−19281.
12. Kishishita, S., Okajima, T., Kim, M., Yamaguchi, H., Hirota, S., Suzuki, S., Kuroda, S., Tanizawa, K., and Mure, M. (2003) Role of copper ion in bacterial copper amine oxidase: spectroscopic and crystallographic studies of metal-substituted enzymes, *J. Am. Chem. Soc. 125*, 1041−1055.
13. Leslie, A. G. W. (1992) *Joint CCP4 and EESF-EACMB newsletter on protein crystallography*, SERC Daresbury Laboratory, Warrington, U.K.
14. Collaborative Computational Project Number 4 (1994) The CCP 4 suite: programs for protein crystallography, *Acta Crystallogr. D 50*, 760−763.
15. Brünger, A. T. (1992) *X-PLOR, Version 3.1. A system for crystallography and NMR*, Yale University Press, New Haven, CT.
16. Ruggiero, C. E., and Dooley, D. M. (1999) Stoichiometry of the topa quinone biogenesis reaction in copper amine oxidases, *Biochemistry 38*, 2892−2898.
17. Nakamura, N., Matsuzaki, R., Choi, Y. H., Tanizawa, K., and Sanders-Loehr, J. (1996) Biosynthesis of topa quinone cofactor in bacterial amine oxidases. Solvent origin of C-2 oxygen determined by Raman spectroscopy, *J. Biol. Chem. 271*, 4718−4724.
18. Suzuki, S., Sakurai, T., Nakahara, A., Manabe, T., and Okuyama, T. (1983) Effect of metal substitution on the chromophore of bovine serum amine oxidase, *Biochemistry 22*, 1630−1635.
19. Matsunami, M., Okajima, T., Hirota, S., Yamaguchi, H., Hori, H., Mure, M., Kuroda, S., and Tanizawa, K. (2004) Chemical rescue of a site-specific mutant of bacterial copper amine oxidase for generation of the topa quinone cofactor, *Biochemistry 43*, 2178−2187.
20. Dove, J. E., Schwartz, B., Williams, N. K., and Klinman, J. P. (2000) Investigation of spectroscopic intermediates during copper-binding and TPQ formation in wild-type and active-site mutants of a copper-containing amine oxidase from yeast, *Biochemistry 39*, 3690−3698.
21. Schwartz, B., Dove, J. E., and Klinman, J. P. (2000) Kinetic analysis of oxygen utilization during cofactor biogenesis in a copper-containing amine oxidase from yeast, *Biochemistry* 39, 3699−3707.
22. Ling, K. Q., and Sayre, L. M. (2005) A dopaquinone model that mimics the water addition step of cofactor biogenesis in copper amine oxidases, *J. Am. Chem. Soc. 127*, 4777−4784.
23. Huheey, J. E. (1972) *Inorganic Chemistry, Principles of Structure and Reactivity*, p 214, Harper & Row, New York.
24. Dubois, J. L., and Klinman, J. P. (2005) Mechanism of post-translational quinone formation in copper amine oxidases and its relationship to the catalytic turnover, *Arch. Biohem. Biophys. 433*, 255−265.
25. Schwartz, B., Olgin, A. K., and Klinman, J. P. (2001) The role of copper in topa quinone biogenesis and catalysis, as probed by azide inhibition of a copper amine oxidase from yeast, *Biochemistry 40*, 2954−2963.
26. Mills, S. A., Goto, Y., Su, Q., Plastino, J., and Klinman, J. P. (2002) Mechanistic comparison of the cobalt-substituted and wild-type copper amine oxidase from *Hansenula polymorpha*, *Biochemistry 41*, 10577−10584.

BI051070R